

Universality of Capillary Rising in Corners

Jiajia Zhou^{1†}, and Masao Doi^{1‡},

¹Center of Soft Matter Physics and its Applications, Beihang University, Beijing 100191, China

(Received xx; revised xx; accepted xx)

We study the dynamics of capillary rising in corners. Using Onsager principle, we derive a partial differential equation that describes the time evolution of meniscus profile. We obtain both numerical solutions and self-similar solutions to this partial differential equation. Our results show that the advance of the meniscus front follows a time-scaling of $t^{1/3}$, in agreement with the experimental results and theoretical conjecture of Ponomarenko *et al.*

1. Introduction

It is well-known that when a capillary tube is brought in contact with a wetting fluid, the fluid rises in the tube and eventually reaches the Jurin's height (de Gennes *et al.* 2004). A related setup is when a cornered geometry consisting of two intersecting plates is brought in contact with the fluid. In this case, a finger-like fluid quickly forms and flows along the corner. The earliest study of the capillary rising in corners can be dated back to the 18th century: Taylor conducted experiments on the fluid rising in a small-angle corner formed by two nearly parallel plates. He identified that the equilibrium shape of the meniscus is a hyperbola (Taylor 1710). In the paper right after Taylor's, Hauksbee (1710) confirmed and quantified Taylor's observation. Other reports on the equilibrium meniscus can be found in works of Langbein (1990) and Finn (1999, 2002).

Even though the equilibrium theory of the meniscus in a cornered geometry is well-established, the understanding on the dynamics was quite recent. The time evolution of the meniscus is governed by several factors. The driving force is the capillary forces which tend to minimize the interfacial energy, and the wetting fluid tends to maximize its coverage on the solid surfaces. The rising of the fluid is hindered by the viscous friction and the gravity. In situations when the gravity can be ignored, the propagation of the meniscus front obeys the classical Lucas-Washburn's $t^{1/2}$ scaling (Lucas 1918; Washburn 1921; Dong & Chatzis 1995; Weislogel & Lichter 1998). When gravity is considered, the meniscus rises with a different $t^{1/3}$ scaling. This result was first derived by Tang & Tang (1994). Higuera *et al.* (2008) developed a more complete theory for the case of two vertical plates forming a small angle. They derived a partial differential equation for the time evolution of the meniscus shape at the late stage based on the lubrication approximation, and derived the $t^{1/3}$ scaling law from this equation. Ponomarenko *et al.* (2011) conducted experiments of capillary rising in corners of different geometries (linear, quadratic and cubic). The universality of the $t^{1/3}$ scaling was demonstrated experimentally. They made a theoretical conjecture, but a rigorous proof is still lacking.

In this paper, we study the dynamics of capillary rising at a general corner. Using Onsager principle (Doi 2013), we derive a partial differential equation that describes the time evolution of meniscus profile. We obtain both numerical solutions and self-similar solutions to the partial differential equation. Our results show that the advance of the

† Email address for correspondence: jjzhou@buaa.edu.cn

‡ Email address for correspondence: masao.doi@buaa.edu.cn

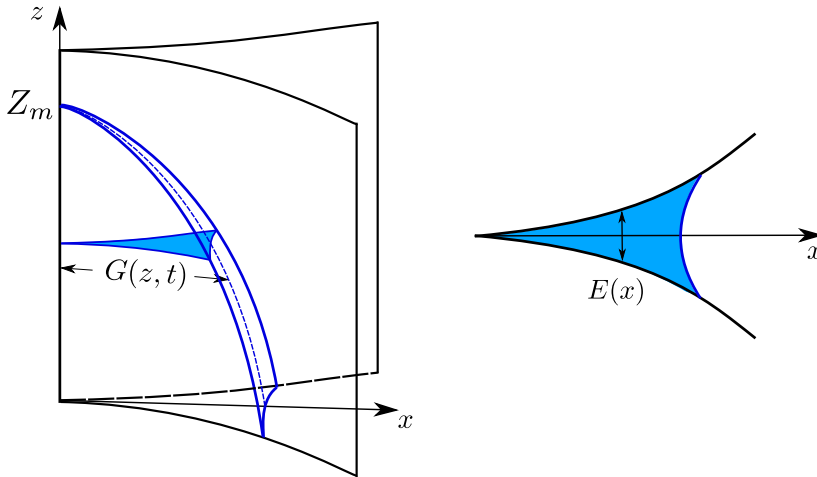


FIGURE 1. Schematic picture of the capillary rising in a corner.

meniscus front follows a time-scaling of $t^{1/3}$, and this scaling is universal for the general power-law corners.

2. Capillary rising in a corner

We consider the capillary rising in a cornered geometry shown in figure 1. The two surfaces forming the corner are described by a function $E(x)$. The coordinate system is set as the z -axis lies on the intersection of the two surfaces, while x -axis bisects the corner. The meniscus is described by its profile in the x - z plane, given by the function $G(z, t)$. The bottom of the meniscus is located at $z = 0$ and in contact with the fluid reservoir. The tip of the meniscus is denoted by $z = Z_m$.

In the plane perpendicular to z -axis, the arc length of the contact between the fluid and the surface is

$$L(G) = \int_0^G dx \sqrt{1 + \frac{1}{4} \left(\frac{dE}{dx} \right)^2}. \quad (2.1)$$

The cross-section area is given by

$$A(G) = \int_0^G dx E(x). \quad (2.2)$$

2.1. Free energy

The free energy of the system is given by

$$F = \int_0^{Z_m} dz \left(\rho g A[G(z, t)] z - 2L[G(z, t)] \gamma \cos \theta \right). \quad (2.3)$$

The first term is the gravitational energy where ρ is the fluid density and g is the gravitational constant. The second term is the interfacial contribution where γ is the surface tension of the fluid and θ is the equilibrium contact angle of the fluid on the solid surfaces. Here we have assumed the two surfaces are close to each so we can neglect the surface energy of the free surface.

The conservation equation is

$$\frac{\partial A}{\partial t} = A' \dot{G} = -\frac{\partial Q}{\partial z}, \quad (2.4)$$

where the prime denotes the derivative with respect to G , $A' = \partial A / \partial G$, and $Q(z, t)$ is the volume flux along the z -axis.

The change rate of the free energy is

$$\dot{F} = \int_0^{Z_m} dz \left(\rho g A' z - 2L' \gamma \cos \theta \right) \dot{G} = \int_0^{Z_m} dz \left(\rho g - 2 \frac{\partial(L'/A')}{\partial z} \gamma \cos \theta \right) Q. \quad (2.5)$$

where we have used the conservation equation (2.4) and the integration by part.

The equilibrium meniscus has a shape determined by

$$\frac{\partial(L'/A')}{\partial z} = \frac{\rho g}{2\gamma \cos \theta}. \quad (2.6)$$

2.2. Dissipation function

The dissipation function is calculated by the lubrication approximation. From the geometry setup, the flow is quasi-2D because the length scale perpendicular to the x - z plane is small. The velocity is then denoted by $\mathbf{v} = (v_x, v_z)$ and is given by Darcy's law

$$\mathbf{v} = -\frac{12E^2}{\eta} \nabla p, \quad (2.7)$$

where ∇ is assumed to be two-dimensional. In general, $v_z \gg v_x$, so the flow is further simplified to be one-dimensional

$$v_z(x, z, t) = C(z, t) E^2(x). \quad (2.8)$$

The flux is an area integration of the local velocity

$$Q(z) = \int_0^{G(z)} dx E(x) v_z(x, z, t) = \int_0^{G(z)} dx E^3(x) C(z, t) = B(G) C(z, t), \quad (2.9)$$

where the function $B(G)$ is given by

$$B(G) = \int_0^G dx E^3(x). \quad (2.10)$$

The velocity is then given by equations (2.8) and (2.9)

$$v_z(x, z, t) = \frac{Q(z)}{B} E^2(x). \quad (2.11)$$

The dissipation function is

$$\Phi = \frac{1}{2} \int_0^{Z_m} dz \int_0^{G(z)} dx \frac{12\eta}{E(x)} v_z^2(x, z, t) = \frac{1}{2} \int_0^{Z_m} dz \frac{12\eta}{B} Q^2(z). \quad (2.12)$$

2.3. Time evolution equation

The Rayleighian of the system is the summation of the change rate of the free energy (2.5) and the dissipation function (2.12)

$$\mathcal{R} = \dot{F} + \Phi = \int_0^{Z_m} dz \left(\rho g - 2 \frac{\partial(L'/A')}{\partial z} \gamma \cos \theta \right) Q + \frac{1}{2} \int_0^{Z_m} dz \frac{12\eta}{B} Q^2. \quad (2.13)$$

The time evolution equation is derived from the Onsager principle, $\delta\mathcal{R}/\delta Q = 0$,

$$Q = \frac{B}{12\eta} \left(-\rho g + 2\gamma \cos \theta \frac{\partial(L'/A')}{\partial z} \right). \quad (2.14)$$

Combined with the conservation equation (2.4), we obtain the time evolution of the meniscus

$$\frac{\partial G}{\partial t} = \frac{1}{A'} \frac{\partial}{\partial z} \left[\frac{B}{12\eta} \left(\rho g - 2\gamma \cos \theta \frac{\partial(L'/A')}{\partial z} \right) \right]. \quad (2.15)$$

3. Power-law corner

We consider an general corner formed by two surfaces which are power n of x

$$E(x) = cx^n, \quad n \geq 1. \quad (3.1)$$

Note here c has a dimension of $[\text{LENGTH}]^{-n+1}$. To derive the time evolution equation, we need the following

$$B(G) = \frac{c^3}{3n+1} G^{3n+1}, \quad (3.2)$$

$$A'(G) = cG^n, \quad (3.3)$$

$$\frac{\partial(L'/A')}{\partial z} \simeq -\frac{n}{cG^{n+1}} \frac{\partial G}{\partial z}. \quad (3.4)$$

We have kept only terms of lowest order.

The flux (2.14) becomes

$$Q = \frac{c^3}{12\eta(3n+1)} G^{3n+1} \left(-\rho g - \frac{2n\gamma \cos \theta}{c} \frac{1}{G^{n+1}} \frac{\partial G}{\partial z} \right). \quad (3.5)$$

The time evolution equation (2.15) becomes

$$\frac{\partial G}{\partial t} = \frac{c^2}{12\eta(3n+1)G^n} \frac{\partial}{\partial z} \left[G^{3n+1} \left(\rho g + \frac{2n\gamma \cos \theta}{c} \frac{1}{G^{n+1}} \frac{\partial G}{\partial z} \right) \right]. \quad (3.6)$$

Scaling the length and the time with the following constants

$$H_c = \left(\frac{2n\gamma \cos \theta}{c\rho g} \right)^{1/(n+1)}, \quad t_c = \frac{12\eta}{c^2\rho g H_c^{2n-1}}, \quad (3.7)$$

we convert the equation into dimensionless form

$$\frac{\partial \tilde{G}}{\partial \tilde{t}} = \frac{1}{(3n+1)\tilde{G}^n} \frac{\partial}{\partial \tilde{z}} \left[\tilde{G}^{3n+1} \left(1 + \frac{1}{\tilde{G}^{n+1}} \frac{\partial \tilde{G}}{\partial \tilde{z}} \right) \right] \quad (3.8)$$

$$= \tilde{G}^{2n} \frac{\partial \tilde{G}}{\partial \tilde{z}} + \frac{2n}{3n+1} \tilde{G}^{n-1} \left(\frac{\partial \tilde{G}}{\partial \tilde{z}} \right)^2 + \frac{1}{3n+1} \tilde{G}^n \frac{\partial^2 \tilde{G}}{\partial \tilde{z}^2}, \quad (3.9)$$

where the tildes denote the corresponding dimensionless variables. This is the generalization of the equation which Higuera *et al.* (2008) derived for the capillary rising in the corner made of planes.

The equilibrium profile is then given by

$$1 + \frac{1}{\tilde{G}^{n+1}} \frac{\partial \tilde{G}}{\partial \tilde{z}} = 0 \quad \Rightarrow \quad \tilde{G} = (n\tilde{z})^{-1/n}. \quad (3.10)$$

The time evolution equation (3.9) admits a self-similar solution of the form

$$\tilde{G}(\tilde{z}, \tilde{t}) = F(\chi)\tilde{t}^\alpha, \quad \chi = \tilde{z}\tilde{t}^\beta, \quad (3.11)$$

where α and β are parameters to be determined. Using the above expressions, we rewrite equation (3.9) as

$$(\beta\chi F' + \alpha F)\tilde{t}^{\alpha-1} = F^{2n}F'\tilde{t}^{(2n+1)\alpha+\beta} + \left(\frac{2n}{3n+1}F^{n-1}(F')^2 + \frac{1}{3n+1}F^nF'' \right) \tilde{t}^{(n+1)\alpha+2\beta}. \quad (3.12)$$

The above equation becomes time-independent if

$$\alpha - 1 = (2n + 1)\alpha + \beta = (n + 1)\alpha + 2\beta, \quad (3.13)$$

which leads to

$$\alpha = -\frac{1}{3n}, \quad \beta = -\frac{1}{3}. \quad (3.14)$$

Equation (3.12) then becomes an ordinary differential equation

$$F^{2n}F' + \frac{2n}{3n+1}F^{n-1}(F')^2 + \frac{1}{3n+1}F^nF'' + \frac{1}{3}(\chi F' + \frac{1}{n}F) = 0. \quad (3.15)$$

The meniscus profile should converge to the equilibrium form $(n\tilde{z})^{-1/n}$ in the limit $\tilde{t} \rightarrow \infty$. This leads to the first boundary condition

$$\chi \rightarrow 0, \quad F(\chi) \rightarrow (n\chi)^{-1/n}. \quad (3.16)$$

The second boundary condition is that the profile $F(\chi)$ approaches zero at certain value $\chi = \chi_0$. Assuming $F(\chi)$ behaves like $(\chi_0 - \chi)^\gamma$ as $\chi \rightarrow \chi_0^-$, each term in equation (3.15) behaves like

$$F^{2n}F' \sim (\chi_0 - \chi)^{(2n+1)\gamma-1}, \quad (3.17)$$

$$F^{n-1}(F')^2 \sim (\chi_0 - \chi)^{(n+1)\gamma-2}, \quad (3.18)$$

$$F^nF'' \sim (\chi_0 - \chi)^{(n+1)\gamma-2}, \quad (3.19)$$

$$\chi F' \sim \chi_0(\chi_0 - \chi)^{\gamma-1}, \quad (3.20)$$

$$F \sim (\chi_0 - \chi)^\gamma. \quad (3.21)$$

Anticipating $\gamma \leq 1$, the dominating terms are $F^{n-1}(F')^2$, F^nF'' , and χF . Upon ignoring other terms, equation (3.15) becomes

$$\frac{2n}{3n+1}F^{n-1}(F')^2 + \frac{1}{3n+1}F^nF'' + \frac{1}{3}\chi_0F' = 0. \quad (3.22)$$

The solution to the above equation leads to the second boundary condition

$$\chi \rightarrow \chi_0, \quad F(\chi) \rightarrow \left[\frac{n(3n+1)}{3(3n-1)}\chi_0(\chi_0 - \chi) \right]^{1/n}. \quad (3.23)$$

Once the solution of (3.15) with the two boundary conditions (3.16) and (3.23) is obtained, we get the asymptotic solution of the tip position

$$\tilde{Z}_m = \chi_0\tilde{t}^{1/3}. \quad (3.24)$$

We can write the above equation with dimensions and scale the length using the capillary length $a_c = \sqrt{\gamma/\rho g}$

$$\frac{Z_m}{a_c} = \chi_0 \left(\frac{n^2 \cos^2 \theta}{3} \right)^{1/3} \left(\frac{\gamma t}{\eta a_c} \right)^{1/3}. \quad (3.25)$$

This result agrees with the conjecture proposed by Ponomarenko *et al.* (2011). In the following, we shall study the numerical solutions for special cases of $n = 1$ and 2.

4. Examples

4.1. linear corner

As a first example, we study the classical example of corner formed by two flat planes. For this case, the $E(x)$ function is given by

$$E(x) = ax, \quad a \ll 1. \quad (4.1)$$

The dimensionless form of the time evolution equation (3.9) is

$$\frac{\partial \tilde{G}}{\partial \tilde{t}} = \frac{1}{4\tilde{G}} \frac{\partial}{\partial \tilde{z}} \left[\tilde{G}^4 \left(1 + \frac{1}{\tilde{G}^2} \frac{\partial \tilde{G}}{\partial \tilde{z}} \right) \right] = \tilde{G}^2 \frac{\partial \tilde{G}}{\partial \tilde{z}} + \frac{1}{2} \left(\frac{\partial \tilde{G}}{\partial \tilde{z}} \right)^2 + \frac{1}{4} \tilde{G} \frac{\partial^2 \tilde{G}}{\partial \tilde{z}^2}. \quad (4.2)$$

This is consistent with Higuera *et al.* (2008) and our previous work (Yu *et al.* 2019).

The equilibrium profile is given by

$$1 + \frac{1}{\tilde{G}^2} \frac{\partial \tilde{G}}{\partial \tilde{z}} = 0 \quad \Rightarrow \quad \tilde{G} = \frac{1}{\tilde{z}}. \quad (4.3)$$

The time evolution equation (4.2) can be solved numerically. The meniscus profiles at different times are shown in figure 2(a). The tip position as a function of time is shown in figure 2(b), which follows a $\tilde{t}^{1/3}$ scaling.

The self-similar solution has the form

$$\tilde{G}(\tilde{z}, \tilde{t}) = F(\chi) \tilde{t}^{-1/3}, \quad \chi = \tilde{z} \tilde{t}^{-1/3}. \quad (4.4)$$

The self-similar solution satisfies the equation (3.15) with $n = 1$

$$F^2 F' + \frac{1}{2} (F')^2 + \frac{1}{4} F F'' + \frac{1}{3} (\chi F)' = 0, \quad (4.5)$$

and the following boundary conditions

$$\chi \rightarrow 0, \quad F(\chi) \rightarrow 1/\chi, \quad (4.6)$$

$$\chi \rightarrow \chi_0, \quad F(\chi) \rightarrow \frac{2}{3} \chi_0 (\chi_0 - \chi). \quad (4.7)$$

The numerical result of the self-similar solution is shown in figure 2(c), which gives

$$\chi_0 \simeq 1.8008. \quad (4.8)$$

4.2. quadratic corner

We next examine the corner formed by two surfaces which are quadratic functions of x

$$E(x) = bx^2. \quad (4.9)$$

Note here b has a dimension of $[\text{LENGTH}]^{-1}$. The dimensionless form of the time evolution equations is

$$\frac{\partial \tilde{G}}{\partial \tilde{t}} = \frac{1}{7\tilde{G}^2} \frac{\partial}{\partial \tilde{z}} \left[\tilde{G}^7 \left(1 + \frac{1}{\tilde{G}^3} \frac{\partial \tilde{G}}{\partial \tilde{z}} \right) \right] = \tilde{G}^4 \frac{\partial \tilde{G}}{\partial \tilde{z}} + \frac{4}{7} \tilde{G} \left(\frac{\partial \tilde{G}}{\partial \tilde{z}} \right)^2 + \frac{1}{7} \tilde{G}^2 \frac{\partial^2 \tilde{G}}{\partial \tilde{z}^2}. \quad (4.10)$$

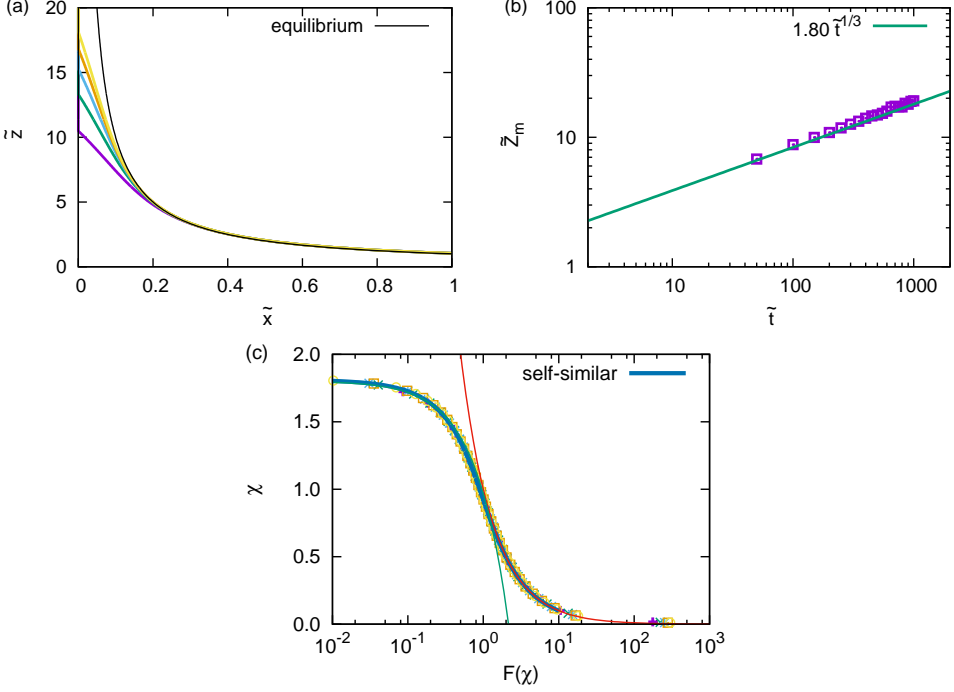


FIGURE 2. (a) Meniscus shape at different times ($\tilde{t} = 200, 400, 600, 800, 1000$ from bottom to top) for the linear corner. The solution are obtained by solving the time evolution equation (4.2). (b) The position of the tip as a function of time. (c) Self-similar solution of equation (4.5). Also shown are the meniscus shapes at different times (shown as symbols) and boundary conditions (4.6, red) and (4.7, green).

The equilibrium profile is given by

$$1 + \frac{1}{\tilde{G}^3} \frac{\partial \tilde{G}}{\partial \tilde{z}} = 0 \quad \Rightarrow \quad \tilde{G} = (2\tilde{z})^{-1/2}. \quad (4.11)$$

The time evolution of the profile is shown in figure 3(a). The tip position as a function of time is shown in figure 3(b), which also follows a $\tilde{t}^{1/3}$ scaling.

The time evolution equation (4.10) admits a self-similar solution of the form

$$G(z, t) = F(\chi)t^{-1/6}, \quad \chi = zt^{-1/3}. \quad (4.12)$$

The solution satisfies the equation

$$F^4 F' + \frac{4}{7} F (F')^2 + \frac{1}{7} F^2 F'' + \frac{1}{3} (\chi F' + \frac{1}{2} F) = 0. \quad (4.13)$$

The boundary conditions are

$$\chi \rightarrow 0, \quad F(\chi) \rightarrow (2\chi)^{-1/2} \quad (4.14)$$

$$\chi \rightarrow \chi_0, \quad F(\chi) \rightarrow \left[\frac{14}{15} \chi_0 (\chi_0 - \chi) \right]^{1/2}. \quad (4.15)$$

The self-similar solution is shown in figure 3(c), which gives

$$\chi_0 \simeq 1.0613. \quad (4.16)$$

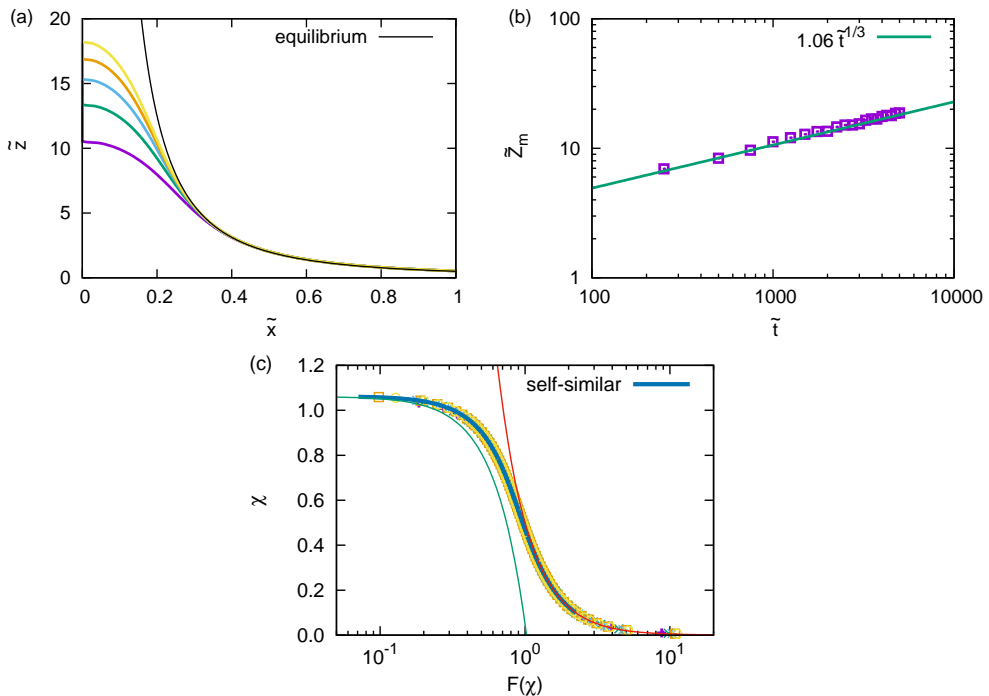


FIGURE 3. (a) Meniscus shape at different times ($\tilde{t} = 1000, 2000, 3000, 4000, 50000$ from bottom to top) for the quadratic corner. The solution are obtained by solving the time evolution equation (4.10). (b) The position of the tip as a function of time. (c) Self-similar solution of equation (4.13). Also shown are the meniscus shapes at different times (shown as symbols) and boundary conditions (4.14, red) and (4.15, green).

5. Conclusion

We have studied the capillary rising of wetting fluid in corners. For corners with small opening angle, we used the Onsager principle and derived a time evolution equation for the meniscus profile for general power-law corners. The time evolution equation has a self-similar solution, and we have showed that the advance of the meniscus front follows a universal $t^{1/3}$ law. The universality of the $t^{1/3}$ scaling was previously demonstrated in experiments (Ponomarenko *et al.* 2011). Here we have shown explicitly that the $t^{1/3}$ scaling is indeed satisfied for general power-law corners.

This work was supported by the National Natural Science Foundation of China (NSFC) through the Grant No. 21774004. M.D. acknowledges the financial support of the Chinese Central Government in the Thousand Talents Program.

REFERENCES

- DOI, MASAO 2013 *Soft Matter Physics*. Oxford University Press.
- DONG, M. & CHATZIS, I. 1995 The imbibition and flow of a wetting liquid along the corners of a square capillary tube. *J. Colloid Interface Sci.* **172**, 278–288.
- FINN, ROBERT 1999 Capillary surface interfaces. *Notices of AMS* **46**, 770–781.
- FINN, ROBERT 2002 Some properties of capillary surfaces. *Milan Journal of Mathematics* **70**, 1–23.
- DE GENNES, PIERRE-GILLES, BROCHARD-WYART, FRANÇOISE & QUÉRÉ, DAVID 2004 *Capillarity and Wetting Phenomena*. Springer.

- HAUKSBEE, FRANCIS 1710 X. an account of an experiment touching the ascent of water between two glass planes, in an hyperbolick figure. *Philos. Trans. R. Soc. London* **27**, 539–540.
- HIGUERA, F. J., MEDINA, A. & LIÑÁN, A. 2008 Capillary rise of a liquid between two vertical plates making a small angle. *Phys. Fluids* **20**, 102102.
- LANGBEIN, DIETER 1990 The shape and stability of liquid menisci at solid edges. *J. Fluid Mech.* **213**, 251.
- LUCAS, R. 1918 Ueber das zeitgesetz des kapillaren aufstiegs von flüssigkeiten. *Kolloid-Zeitschrift* **23**, 15–22.
- PONOMARENKO, ALEXANDRE, QUÉRÉ, DAVID & CLANET, CHRISTOPHE 2011 A universal law for capillary rise in corners. *J. Fluid Mech.* **666**, 146–154.
- TANG, LEI-HAN & TANG, YU 1994 Capillary rise in tubes with sharp grooves. *J. Phys. II* **4**, 881–890.
- TAYLOR, BROOK 1710 IX. part of a letter from mr. brook taylor, f. r. s. to dr. hans sloane r. s. secr. concerning the ascent of water between two glass planes. *Phil. Trans. R. Soc. London* **27**, 538–538.
- WASHBURN, EDWARD W. 1921 The dynamics of capillary flow. *Phys. Rev.* **17**, 273–283.
- WEISLOGEL, MARK M. & LICHTER, SETH 1998 Capillary flow in an interior corner. *J. Fluid Mech.* **373**, 349–378.
- YU, TIAN, JIANG, YING, ZHOU, JIAJIA & DOI, MASAO 2019 Dynamics of Taylor rising. *Langmuir* **35**, 5183–5190.